Nat Struct Mol Biol. Author manuscript; available in PMC 2016 August 03.

Published in final edited form as:
Nat Struct Mol Biol. 2013 July ; 20(7): 851–858. doi:10.1038/nsmb.2598.

Bimodal expression of *PHO84* is modulated by early termination of antisense transcription

Manuele Castelnuovo[1,3], **Samir Rahman**[2,3], **Elisa Guffanti**[1,3], **Valentina Infantino**[1], **Françoise Stutz**[1,4], and **Daniel Zenklusen**[2,4]

[1]Department of Cell Biology and National Center of Competence in Research "Frontiers in Genetics", University of Geneva, Switzerland [2]Département de Biochimie, Université de Montréal, Canada

Abstract

Many *S. cerevisiae* genes encode antisense transcripts some of which are unstable and degraded by the exosome component Rrp6. Loss of Rrp6 results in the accumulation of long *PHO84* antisense RNAs and repression of sense transcription through *PHO84* promoter deacetylation. We used single molecule resolution fluorescent in situ hybridization (smFISH) to investigate antisense-mediated transcription regulation. We show that *PHO84* antisense RNA acts as a bimodal switch, where continuous low frequency antisense transcription represses sense expression within individual cells. Surprisingly, antisense RNAs do not accumulate at the *PHO84* gene but are exported to the cytoplasm. Furthermore, loss of Rrp6, rather than stabilizing *PHO84* antisense RNA, promotes antisense elongation by reducing its early transcription termination by Nrd1-Nab3-Sen1. These observations suggest that *PHO84* silencing results from constant low frequency antisense transcription through the promoter rather than its static accumulation at the repressed gene.

Keywords

yeast; single molecule FISH; antisense RNA; Rrp6; Nrd1-Nab3-Sen1; transcription termination; antisense 3′ end processing; *PHO84* regulation

Introduction

Genome-wide pervasive transcription has been reported in many eukaryotic organisms, producing hundreds of non protein-coding RNAs (ncRNAs). Even the small yeast genome encodes many intergenic, promoter-associated and antisense transcripts, some stable and

[4]Corresponding authors: francoise.stutz@unige.ch, daniel.r.zenklusen@umontreal.ca.
[3]Equal contribution

Author Contribution
MC performed ChiP and RNA analyses; SR performed the smFISH experiments; EG prepared strains and performed RNA analyses; VI made mutants and RNA analyses. MC, SR, DZ and FS analyzed that data; DZ and FS supervised the project and wrote the manuscript.

others rapidly degraded and hence called cryptic unstable transcripts (CUTs) [1–3]. The degradation of these 200–600 bases long CUTs is in great part mediated by Rrp6, a 3′–5′ exonuclease belonging to the nuclear exosome [4,5]. Exosome-mediated degradation is assisted by TRAMP, a surveillance complex containing the non-canonical polyA polymerase Trf4, while mRNAs are polyadenylated by Pap1, resulting in stable and export competent mRNPs [4,6–9].

The Nrd1-Nab3-Sen1 (NNS) complex mediates transcription termination of CUTs, snRNA, snoRNAs, and some mRNAs [7,10–13]. It is recruited to the 5′end of most RNA polymerase II (RNAPII) transcription units through interaction of Nrd1 with the Ser5/Ser7 phosphorylated RNAPII C-terminal domain (CTD) [14–16]. Transcription termination by NNS depends on the abundance of specific Nrd1 and Nab3 binding motifs on the nascent RNA and occurs primarily on short transcripts as the recruitment of NNS decreases towards the 3′ end of long transcription units. Consistent with the physical interactions between the NNS, TRAMP and exosome complexes, CUT degradation has been directly linked to NNS-mediated early termination [4,7,10,11].

Genome-wide studies indicate that numerous genes produce upstream tandem or antisense transcripts [17,18], a fraction of which may function in gene regulation [19]. Transcription of an upstream tandem ncRNA was proposed to interfere with the expression of the *SER3* [20,21], *URA2* [22], *FLO11* [23] and *IME1* [24] genes through various mechanisms, including co-transcriptional chromatin modifications, that establish histone repositioning and a repressive chromatin state blocking access to transcription factors. While the *RME2* antisense RNA was proposed to repress the meiotic regulator *IME4* gene *via* transcription interference [25,26], antisense RNA transcription may also affect sense expression by influencing the epigenetic state of chromatin. Indeed, antisense RNA transcription originating within *GAL10* and running into the divergent *GAL1* gene in glucose deposits H3K4-me2/3 and H3K36-me3 by the Set1 and Set2 histone methyl transferases respectively. These marks signal the recruitment of the Rpd3S histone deacetylase (HDAC) attenuating *GAL1* gene expression [27,28]. H3K4me2 deposited by Set1 during noncoding transcription was also implicated in repression by signaling the recruitment of the Rpd3L and Set3 histone deacetylases to specific gene promoters [24,29,30].

Our earlier studies focused on the *PHO84* gene encoding a high-affinity phosphate transporter. *PHO84* transcription is induced by the activator Pho4 imported into the nucleus upon phosphate starvation [31]. The activation threshold of the *PHO84* promoter depends on the nuclear concentration of Pho4 and the accessibility of the Pho4 binding sites [32,33]. *PHO84* mRNA is weakly expressed in standard yeast media containing intermediate phosphate levels. In these conditions, *PHO84* also produces two antisense transcripts (*PHO84* AS) starting at its 3′ end and extending into the *PHO84* promoter. Loss of Rrp6 increases *PHO84* AS levels and this accumulation is paralleled by the recruitment of the Hda1/2/3 histone deacetylase (HDAC) complex over the locus, histone deacetylation at the promoter and transcriptional repression. We proposed that stabilization and accumulation of antisense RNAs at the *PHO84* gene might facilitate Hda1 recruitment maintaining repression of sense transcription [34].

To further elucidate the mechanism of antisense-mediated transcription regulation, we used single molecule fluorescent *in situ* hybridization (smFISH) to detect individual sense and antisense RNAs [35–37]. We show that the presence of *PHO84* sense and antisense transcripts in single cells is strongly anti-correlated, suggesting a switch-like regulation mechanism. Our data provide evidence that Rrp6 does not degrade full-length antisense transcripts, but prevents antisense transcription elongation by favoring early termination by Nrd1-Nab3-Sen1, while the H3K4 methyl transferase Set1 may antagonize this event. These observations suggest that antisense-mediated silencing is regulated, at least in part, through transcription attenuation and that *PHO84* repression results from antisense transcription through the promoter, followed by rapid export of antisense RNA into the cytoplasm.

Results

Bimodal expression of *PHO84* sense and antisense transcripts

We have suggested that *PHO84* AS RNAs might stably associate, possibly in multiple copies, with the *PHO84* gene to help efficient recruitment of chromatin modifiers. Such a process would require only a single initial burst of antisense transcription to establish silencing of sense. Conflicting with such a model, Northern blot analysis of *PHO84* sense and antisense expression shows that low levels of antisense RNA can be detected in wild-type cells under conditions where *PHO84* sense is transcribed, indicating that very low expression of antisense might not be sufficient to repress sense transcription (Fig. 1a). Alternatively, low level of *PHO84* AS RNA expression in wild-type cells may continuously fine-tune *PHO84* sense expression, a process that may be regulated by Rrp6. However, different levels of antisense expression in wild-type versus *Δrrp6* cells may also reflect different subclasses of cells in a population that express either *PHO84* sense or antisense. Different models can therefore be suggested for how antisense-mediated silencing of the *PHO84* gene is established. Either the regulation occurs by a graded response, where increasing antisense levels lead to decreasing levels of sense transcription, or by a switch-like mechanism, where low level of antisense expression in a single cell is sufficient to down-regulate sense transcription (Fig. 1b).

To detect single RNA molecules, we designed smFISH probes targeted to the 5′ region of sense and antisense *PHO84* transcripts. Probes were labeled with fluorescent dyes allowing to distinguish sense and antisense transcripts and hybridized to fixed yeast cells, followed by image acquisition. We first localized *PHO84* transcripts in wild-type cells under conditions where both sense and antisense RNAs are detected by Northern blotting (Fig. 1a). While both *PHO84* sense and antisense RNAs can be detected in wild-type cells (Fig. 1c), they are never co-expressed (Fig. 1d), suggesting that antisense-mediated repression of *PHO84* operates through a switch-like rather than a graded process. Consistent with the role of Rrp6 in modulating sense repression through antisense RNA, the fraction of cells expressing antisense increases (from 28 to 55%) in a *Δrrp6* strain, whereas the percentage of sense expressing cells decreases (Fig. 1c, 1d and 1e).

At the single cell level, sense expression is much higher than antisense: large numbers of *PHO84* mRNAs are detected within individual cells suggesting that *PHO84* transcription occurs in strong bursts when repression is overcome. In contrast, *PHO84* AS expression

levels are very low in individual wild-type cells, with most cells expressing no or only a single antisense RNA molecule. In the *Δrrp6* strain, antisense levels are higher and more cells express *PHO84* AS, however most cells still only contain 1–3 antisense RNA molecules and a substantial fraction of cells (40%) shows no signal (Fig. 1c, 1d and 1e). Double negative cells are not due to inability to detect RNAs in these cells, as double staining for the constitutively expressed *MDN1* RNAs shows expression of *MDN1* in all cells (Supplementary Fig. 1a). Thus, very low antisense expression appears sufficient to exert a repressive effect on *PHO84* transcription in individual cells. Unexpectedly, we did not observe a significant accumulation of antisense RNA in the nucleus (Fig. 2) as most antisense RNAs detected in wild-type and *Δrrp6* cells are found in the cytoplasm, suggesting that *PHO84* AS RNAs, like mRNAs, do not remain associated with the *PHO84* gene but are rapidly exported.

PHO84 antisense RNAs do not accumulate at the *PHO84* locus

The fraction of antisense RNA molecules detected in the nucleus can represent nascent RNAs associated with the transcription machinery, RNAs diffusing in the nucleoplasm on their way to the cytoplasm, or antisense RNAs associated with the *PHO84* gene in a transcription independent manner. To distinguish between these possibilities, we further characterized the nuclear *PHO84* AS RNA signal. The quantitative nature of smFISH allows defining how many RNAs are present in a single RNA spot and we have shown that cytoplasmic mRNA spots have a uniform signal intensity representing single mRNAs [36,38]. Nuclear signals often show higher intensities as they represent sites of active transcription where multiple nascent mRNAs are associated with a gene. The frequency and number of nascent mRNAs detected for a specific gene depend on its transcription rate and length. If antisense RNAs accumulate in multiple copies at the *PHO84* gene, higher intensity nuclear signals compared to cytoplasmic signals should be detected. Furthermore, if antisense RNAs stay associated at the gene for long periods of time, most cells with no sense expression should show a nuclear antisense signal. As shown in Figures 2a and 2b, nuclear signals corresponding to multiple nascent mRNAs are detected on the long, constitutively transcribed *MDN1* gene, however most nuclear *PHO84* AS RNA signals show the same intensity as single cytoplasmic antisense molecules, indicating that antisense transcripts do not accumulate at the *PHO84* gene. Furthermore, only 13% of WT and 20% of *Δrrp6* cells show nuclear signal, inconsistent with a model where antisense RNAs stay associated with the gene locus for a long time (Fig. 2c).

It is likely that most nuclear AS signals with an intensity of a single RNA represent nascent rather than freely diffusing nucleoplasmic antisense RNAs. Indeed, nuclear *PHO84* AS signals, like nascent *PHO84* mRNA signals are always located at the nuclear periphery, consistent with the subtelomeric position of *PHO84* on chromosome XIII locating the gene close to the nuclear periphery (Supplementary Fig. 1b). Furthermore, our earlier studies showed that mRNAs are rarely detected in the nucleoplasm except at the site of transcription, suggesting that mRNA export is fast, probably occurring within seconds after release from the site of transcription [36,39]. If *PHO84* AS RNAs transcribed at a low frequency behave like mRNAs, detecting antisense RNAs within the nucleus is likely a rare event, except when they are nascent. Thus, nuclear *PHO84* AS RNAs are likely to be

nascent and to behave like mRNAs that rapidly dissociate from the locus after synthesis. These observations suggest that antisense transcription rather than antisense RNA accumulation at the gene may mediate *PHO84* gene silencing.

PHO84 antisense RNAs behave like mRNAs

To confirm that antisense transcripts behave like mRNAs, we first monitored antisense RNA distribution in a mutant for the poly(A) polymerase Pap1. mRNA cleavage and polyadenylation occurs co-transcriptionally and is required for nuclear export. The *pap1-1* and *pap1-1Δrrp6* temperature sensitive strains were grown at 25°C and shifted to 37°C before fixation. After a 1h heat-shock, *pap1-1* cells accumulate antisense RNAs in the nucleus and less transcripts are observed in the cytoplasm, a phenotype that was more pronounced in *pap1-1Δrrp6* (Fig. 3a and 3b). Antisense RNAs do not accumulate in one spot but distribute throughout the nucleus, with a tendency to localize within the nucleolus (Supplementary Fig. 2a). The higher accumulation in *pap1-1 Δrrp6* compared to *pap1-1* suggests that antisense RNAs are degraded by Rrp6 when not polyadenylated by Pap1 and/or that a higher number of antisense RNAs is expressed in a *pap1-1 Δrrp6* background (Fig. 3b, and see below). Loss of the non-canonical polyA polymerases Trf4 and Trf5 did not reduce the amounts of polyadenylated *PHO84* AS RNAs, confirming their polyadenylation by Pap1 (Fig. 3c). Notably, shifting *pap1-1 Δrrp6* double, but not *pap1-1* single, mutant cells to 37°C results in the accumulation of an elongated polyadenylated antisense RNA (Supplementary Fig. 2b). Together, these analyses suggest that when Pap1 is inactive, a single long antisense transcript is produced that remains in the nucleus and is degraded by Rrp6, presumably following polyadenylation by the non-canonical Trf4/5 polyA polymerase as a result of nuclear surveillance [40]. Thus the classical cleavage and polyadenylation machinery is required for 3′ end processing and export of *PHO84* AS RNA confirming that these long ncRNAs behave like mRNAs. Accordingly, their nuclear export is mediated by the general mRNA export receptor Mex67, since *PHO84* AS transcripts accumulate in the nuclei of the *mex67-5* and even more in the *mex67-5Δrrp6* conditional mutants when shifted to 37°C (Supplementary Fig. 3a and 3b). Moreover, the number of cytoplasmic *PHO84* AS RNAs greatly increases in *Δxrn1* cells indicating that, like mRNAs, they undergo 5′ to 3′ exonucleolytic degradation in this compartment (Supplementary Fig. 3c).

Antisense RNA at *PHO84* gene requires active transcription

A feature of *bona fide* mRNAs is their rapid dissociation from the gene after transcription termination; nascent mRNA detection therefore requires ongoing transcription. To define whether detection of nuclear antisense RNAs requires transcription, we determined *PHO84* AS localization and abundance in the *rpb1-1* strain, containing a temperature sensitive mutation in the major RNAPII subunit [41]. To test the efficiency of transcription shutoff we simultaneously monitored *MDN1* mRNA distribution. Figure 4 shows that after 5 min at 37°C, most cells have lost nuclear *MDN1* signal and mRNA abundance further declines over time, consistent with transcription shutoff. Similarly, nuclear *PHO84* AS signal is quickly lost and cytoplasmic RNA numbers subsequently decrease. Thus, ongoing transcription is required to detect nuclear antisense RNA further indicating that *PHO84* AS RNA does not stay associated with the *PHO84* gene. The observation that the number of cells with

antisense RNA increases in *Δrrp6* (Fig. 1d) and that antisense transcription rather than accumulation is required to mediate sense silencing (Fig. 1 and 2) suggest that loss of Rrp6 does not primarily affect antisense RNA stability, but may also influence its transcription.

To compare *PHO84* AS RNA turnover in wild-type and *Δrrp6* cells, we measured antisense levels at various times following inhibition of RNAPII transcription with phenanthroline (Fig. 5a) [42]. Surprisingly, *PHO84* AS RNA decays at a similar rate in both strains with a half-life of 11.4 min in wild-type and 12 min in *Δrrp6* cells (See Methods). In contrast, the half-life increased to 27.3 min in the *Δxrn1* strain, confirming 5′ to 3′ antisense RNA degradation in the cytoplasm as revealed by smFISH (Supplementary Fig. 3c). Since loss of Rrp6 does not substantially increase *PHO84* AS RNA half-life, these results indicate that the elevated levels of antisense RNA in *Δrrp6* (Fig. 5b) are due to increased antisense RNA production rather than stability.

Loss of Rrp6 increases antisense transcription

Increased *PHO84* AS transcription in *Δrrp6* predicts a higher number of nascent antisense RNAs in this strain versus wild type. Indeed, besides an increased number of both antisense producing cells and antisense RNA molecules per cell (Fig. 1e), more *Δrrp6* cells (20%) show nascent antisense RNAs compared to wild type (13%) consistent with higher transcription frequency in *Δrrp6* (Fig. 2c).

One hallmark of active transcription is K4 methylation on histone H3 by Set1, the only yeast H3K4 histone methyl transferase recruited to the 5′ end of transcription units [43,44]. Most active genes show peaks of H3K4 trimethylation at the 5′end, di-methylation in the middle and monomethylation at the 3′end. We postulated that if loss of Rrp6 increases antisense transcription, Set1 dependent H3K4me3 should increase over the *PHO84* 3′ end in *Δrrp6* versus wild type. We performed chromatin immunoprecipitation (ChIP) of tri- and dimethylated H3K4 in wild-type and *Δrrp6* cells also devoid of the transcription factor Pho4, completely abrogating sense transcription (Fig. 5c). In this setup H3K4 methylation derives only from antisense transcription. Interestingly, we observe that the H3K4me3 and H3K4me2 peaks respectively at the 3′ end and middle regions of *PHO84* are substantially increased upon loss of Rrp6. As a control, the *ACT1* gene showed the expected high level of H3K4me3 at its 5′ end with no enrichment at the 3′ end, consistent with the absence of antisense transcription on this gene. Due to the low antisense transcription frequency, RNAPII is barely detectable at the 3′end of *PHO84* in a *Δpho4* strain, yet the levels slightly increase in *Δrrp6Δpho4* (data not shown). The more efficient detection of H3K4 methylation suggests persistence of this histone mark between transcription events. These observations support the view that loss of Rrp6 increases antisense transcription.

PHO84 antisense elongation is regulated by the NNS complex

To investigate how loss of Rrp6 may increase transcription, we explored the physical and functional links of Rrp6 with the Nrd1-Nab3-Sen1 and TRAMP complexes [4,7,11]. Transcription termination by NNS is stimulated by Nrd1 and Nab3 binding motifs on the nascent RNA. Interestingly, several potential Nrd1-Nab3 binding sites are present within the 5′ end of *PHO84* AS RNA (Fig. 6a and Supplementary Fig. 4). Furthermore, transcriptome-

wide analyses of Nrd1-Nab3 bound RNA sequences revealed association with the 5′ end of many antisense transcripts, including *PHO84* AS RNA, suggesting that these ncRNAs undergo early transcription termination [45,46]. Accordingly, depletion of the essential Nrd1 protein using the glucose repressible *GAL1* promoter leads to increased *PHO84* AS levels in wild-type cells and this effect is even more pronounced in *Δrrp6* (Fig. 6b). Moreover, a modified *PHO84* gene in which a number of putative Nrd1-Nab3 binding sites at the 5′ end of the antisense RNA have been mutagenized, produces more antisense transcripts both in wild-type and *Δrrp6* cells. The relatively modest effect of the *cis*-mutations may be due to only partial removal of potential NNS binding sites to maintain the *PHO84* open reading frame intact (Supplementary Fig. 4). These observations confirm the role of Nrd1/Nab3/Sen1 in *PHO84* AS transcription attenuation.

Rrp6 and Set1 have opposite effects on early termination

To address whether absence of Rrp6 might increase antisense transcription elongation by affecting optimal NNS function, we monitored Nrd1 association with the 3′ end of the *PHO84* gene by ChIP in wild-type or *Δrrp6* cells (Fig. 6c). While loss of Rrp6 does not affect Nrd1 protein levels, we observed a large decrease in Nrd1 binding at the *PHO84* 3′ end in *Δrrp6*, suggesting that loss of Rrp6 may affect early termination by lowering the association of Nrd1-Nab3-Sen1. The additive effect on antisense RNA production of *Δrrp6* and Nrd1 depletion or Nrd1-Nab3 binding site mutagenesis (Fig. 6b and Supplementary Fig. 4b), situations that weaken but do not eliminate Nrd1-Nab3-Sen1 function, supports the notion that NNS and Rrp6 act in the same pathway.

Interestingly, Nrd1 association with the *PHO84* 3′ end was slightly enhanced in *Δset1*, suggesting that in contrast to *Δrrp6*, loss of Set1 may increase early termination (Fig. 6c). A recent study similarly reported elevated Nrd1 binding in *Δset1* and correlated this phenotype with increased Ser5 phosphorylated RNAPII CTD, the mark implicated in NNS recruitment [16,47]. This is also in agreement with our earlier data showing reduced *PHO84* AS RNA production in *Δset1* [48]. Accordingly, smFISH analyses indicate reduced antisense expression in *Δset1* and restoration of antisense RNA levels in *Δset1Δrrp6* (Supplementary Fig. 5). Taken together, the data suggest that Rrp6 and Set1 have antagonistic effects in the regulation of antisense RNA production by respectively facilitating and interfering with early transcription termination by Nrd1-Nab3-Sen1.

Discussion

Expanding on an extensive list of *cis*- and *trans*-acting factors, recent studies have established ncRNAs as additional players in controlling the regulated expression of protein coding genes. Transcription regulation by ncRNAs is achieved by multiple ways, however in-depth mechanistic understanding is still missing. Our detailed analyses of *PHO84 cis*-acting antisense RNAs at a single cell and single molecule level indicate that low frequency antisense transcription, but not the antisense RNA itself, contributes to *PHO84* gene repression.

Our earlier studies showed that an extra *PHO84* gene copy induces repression of both the transgene and the endogenous copy, and suggested that *PHO84* AS RNAs may participate in

a still poorly defined mechanism of silencing in *trans* independent of Hda1/2/3 and therefore distinct from silencing in *cis* [48]. Based on the rapid export of antisense RNAs revealed by smFISH, it seems unlikely that antisense RNAs act in *trans* by diffusing from one gene copy to the other, unless the two genes undergo pairing. The primarily cytoplasmic localization of *PHO84* AS RNAs suggests they are more likely to act in *trans* through an indirect mechanism. These possibilities should be investigated in the future.

smFISH reveals distinct sense and antisense expression modes

The single molecule microscopy approach revealed critical parameters on *PHO84* regulation that could not be obtained using classical ensemble measurements (Fig. 1). First, we showed that antisense-mediated regulation does not generate a gradual decrease of sense transcription but modulates the threshold of the *PHO84* activation switch. Second, smFISH revealed that sense and antisense expression are achieved through different modes, *PHO84* mRNA being transcribed in bursts that lead to a strong accumulation in a fraction of cells, whereas antisense RNA is transcribed constantly at a very low rate in most cells not expressing *PHO84* mRNA. Third, the ability to localize individual RNAs within different cellular compartments showed that *PHO84* AS RNA behaves like an mRNA that dissociates from the gene locus after polyadenylation by Pap1, leaves the nucleus using the canonical Mex67-dependent mRNA export pathway, and is eliminated by the cytoplasmic Xrn1-dependent RNA degradation machinery.

Loss of Rrp6 favours antisense transcription elongation

Consistent with the increased levels of antisense RNA observed in *Δrrp6* through classical RNA analyses (Fig 1a), smFISH revealed more antisense RNA molecules per cell as well as an increased number of cells with antisense RNA compared to wild type (Fig. 1d and 1e). Our observations indicate that loss of Rrp6 does not result in nuclear stabilization of full-length antisense RNAs but rather promotes antisense transcription followed by rapid export. First, although the number of cells showing nascent transcripts is increased in *Δrrp6*, more than one molecule is rarely observed at the transcription site; moreover this nuclear signal is strictly dependent on ongoing transcription both in wild type and *Δrrp6* indicating that once made, antisense transcripts don't remain at the gene (Fig. 2, 3 and 4). Second, the antisense RNA turnover rate is comparable in wild-type and *Δrrp6* strains, supporting the view that the increased steady state levels in *Δrrp6* are due to enhanced antisense RNA production (Fig. 5a and 5b). Finally, H3K4 tri- and di-methylation at the 3′ end and middle region of *PHO84* are higher in the absence of Rrp6 consistent with increased antisense transcription (Fig. 5c). Combining mean transcript values and half-life data (Fig. 1 and 5) indicates a *PHO84* AS RNA transcription frequency of only 1 and 3 RNAs per hour in wild-type and *Δrrp6* cells respectively (Supplementary Table 1). These numbers are consistent with the incidence of nascent transcripts, another measure for transcription frequency. In *Δrrp6*, 20% of cells show a nuclear *PHO84* AS signal (Fig. 2c), suggesting that a cell contains a nascent mRNA 20% of the time, i.e. for 12 min every hour. Assuming transcription of antisense RNA occurs at a rate similar to other low frequency transcribed genes (0.8kb/min) and termination/transcript release is a rate-limiting step as suggested for mRNAs, transcription of the 2.3kb antisense RNA takes almost 4 minutes to complete [36]. This fits well with a transcription frequency of 3 *PHO84* AS RNAs per hour, as a nascent antisense signal would be detected 3 times per

hour during 4 min. Consistently, *pap1-1* Δ*rrp6* cells accumulate in average 3.7 AS RNAs after 1 hour heat shock (Fig. 3b). These data indicate that continuous but low frequency antisense RNA transcription occurs in cells not expressing sense.

Rrp6 and Set1 influence antisense early termination by Nrd1

Antisense RNA transcription frequency is increased in Δ*rrp6* compared to wild-type and accompanied by a higher fraction of cells with a repressed *PHO84* gene. Regulating antisense transcription frequency could therefore be a way to modulate the strength of repression. Transcription frequency of *PHO84* AS RNA appears to be controlled both at the level of initiation and through the regulation of elongation and termination efficiency of a short transcript by the NNS complex. It is unclear what controls initiation; the presence of a NFR in the 3′UTR of the *PHO84* gene may be sufficient to allow low frequency transcription of antisense RNA [18]. This 'default' antisense transcription may be further controlled by the NNS termination pathway. Indeed, mutagenesis of Nrd1-Nab3 binding motifs or Nrd1 depletion result in increased antisense levels. Moreover the association of Nrd1 with the *PHO84* 3′ end is strongly reduced in *Δrrp6* suggesting that Rrp6 may contribute to antisense early termination by favouring stable NNS complex association (Fig. 6). Notably, as recently observed [47], Set1 has opposite effects since its loss increases Nrd1 binding (Fig. 6c), suggesting that Set1 and/or H3K4 methylation may interfere with early termination efficiency. These observations are consistent with the positive effect of Set1 and H3K4 trimethylation on antisense RNA production at *PHO84* and other antisense-producing genes [48,49]. Interestingly, both gene-specific and genome-wide studies suggest that TRAMP and exosome components are required for snRNA/snoRNA transcription termination by Nrd1 and loss of Trf4 was shown to reduce Nrd1 binding to snRNA genes [50,51]. Together with our results, these observations support the view that both TRAMP and Rrp6 may more generally contribute to efficient NNS-dependent transcription termination. Since the activity of both Nrd1 and Rrp6 is regulated in different physiological conditions [52,53], genes like *PHO84* may be controlled in part through modulation of antisense transcription elongation.

A novel view on antisense-mediated gene repression

Our data show that *PHO84* transcription is regulated by a sensitive on-off switch where sense transcription is either completely turned off or strongly induced once the repression is overcome. The activation threshold of Pho4 regulated genes is defined both by the nuclear concentration of the Pho4 transcription factor and accessibility of Pho4 binding sites [32]. Antisense transcription may ensure that *PHO84* transcription is activated only in presence of a strong enough stimulus either by reducing Pho4 accessibility through promoter nucleosome rearrangement, and/or, as shown previously, by placing repressive histone marks [34]. Antisense transcription is not able to establish stable repressive marks, as cells rapidly induce *PHO84* sense expression when shifted from high phosphate, a condition where antisense RNA is abundant, to low phosphate medium (Supplementary Fig. 6). Antisense transcription might therefore act as a buffer, protecting cells from responding to weak signals.

H3K4 di-methylation deposited by Set1 during noncoding RNA transcription has been implicated in gene repression [49,54] by recruiting the histone deacetylases Set3 and Rpd3L at

promoter regions [24,29,55]. Notably, we observed that in addition to Hda1, *PHO84* antisense-dependent repression similarly depends on Set1 and Rpd3L (J. Zaugg, M. C., N. Luscombe and F. Stutz, unpublished). Thus, besides promoting antisense production, Set1-dependent H3K4 methylation deposited during antisense transcription may also contribute to *PHO84* gene repression by enhancing HDAC recruitment to the sense promoter.

Recent global studies show that many chromatin regulators, including Set1, barely affect steady state gene expression, but are required for rapid transcriptional responses to environmental stresses. Many of these highly regulated genes are associated with distal or antisense ncRNA transcription [29,30,49]. Consistently, our large-scale search for *PHO84*-like genes, i.e. repressed by antisense transcription in *Δrrp6* in a process dependent on Set1 and the HDACs Rpd3 and Hda1, identified highly regulated TATA-box containing genes (J. Zaugg, M. C., N. Luscombe and F. Stutz unpublished). These genes are frequently expressed in transcription bursts and their promoters undergo important chromatin rearrangements upon activation or repression, as described for *PHO84* [32,33]. Thus, a larger picture emerges suggesting that the role of noncoding transcription may be to reinforce the rapid on-off switch of highly regulated genes by promoting the formation of repressive chromatin. This process occurs in wild-type cells and is enhanced in *Δrrp6*. Further studies will address how, following a sense transcription burst, low rate antisense transcription contributes to efficient nucleosome reassembly at the promoter preventing inappropriate transcription factor binding and firing of sense transcription.

Experimental procedures

Yeast strains, oligo primers and probes used in this study are listed in Supplementary Table 2. Detailed experimental procedures for media, culture conditions, smFISH, RNA extraction, Northern blotting, RTqPCR, ChIP and plasmid constructions are provided in online Methods.

Online Methods

Strains, media and culture conditions

The yeast strains used in this study are listed in Supplementary Table 2. Yeast strains were streaked on YEPD plates at 25°C. Liquid cultures were inoculated with cells taken from plates and grown at 25°C for 16 to 24 h under exponential conditions (OD_{600} < 0.8) in YEPD or synthetic complete (SC) minimum medium.

Fluorescent in situ hybridization

Fluorescent in situ hybridization procedure—20 nucleotides long DNA oligonucleotides containing a single 3′ amine were labeled post synthesis with amine-reactive fluorescent dyes and hybridized to paraformaldehyde fixed yeast cells as described in [36,37]. Images were acquired using epifluorescent microscope and 3D datasets were reduced to 2D datasets for image analysis. Cell segmentation, single RNA counting and quantification of nascent transcripts was done as described in [36].

Probe design and labeling

20 nucleotide long DNA oligonucleotide probes were designed using the online software Stellaris™ Probe Designer version 2.0 at the Biosearch Technologies website. Probes have typically a 50% GC content, however, GC content can range from 40–55% (for probes sequences see Supplementary Table 2). Probes were synthetized containing a single 3′ amine that can be coupled to an amine-reactive fluorescent dye. For a typical labeling reaction, 20ug of pooled probes (31 for *PHO84* antisense, 30 for *PHO84* sense and 48 probes for *MDN1*) were lyophilized and re-suspended in labeling buffer (0.1 M sodium bicarbonate, pH 9.0) and mixed with a single reactive dye pack of amine-reactive dye (DyLight™ amine-reactive dyes: DyLight 550 (#62263), DyLight 594 (#46413), and DyLight 650 (#62266) (Thermo Scientific). The reaction was carried out overnight in the dark at room temperature. Labeled probes were purified using the Quiagen QIAquick Nucleotide Removal columns (Qiagen #28304) according to the manufacturer's instructions. Probe concentration and labeling efficiency were measured using a NanoPhotometer™ Pearl (Implen) and calculated as described in [38]. Probes are stored at −20°C in the dark.

Cell Fixation, Preparation, Storage and Hybridization

Cells were grown in SD complete and 2% glucose at 25°C overnight to mid-log phase (OD600=0.6–0.8) and fixed by adding paraformaldehyde (Electron Microscopy Science #15714) to a final concentration of 4% for 45 min at room temperature. Cells were subsequently washed 3x with 10ml of Buffer B (1.2 M sorbitol, 100 mM KHPO4, pH 7.5) and stored overnight at 4°C in Buffer B. Cell walls were then digested with lyticase (Sigma # L2524, dissolved in 1x PBS to 25,000 U/ml. Stored at −20 C). Digested cells were plated on poly-L-lysine treated coverslips and stored in 70% ethanol at −20°C in 12 well cell culture plates. Cells can be stored in 70% ethanol for several months prior to hybridization. For hybridization, cells were removed from 70% ethanol, washed twice with 2x SSC, and hydrated in 10% Formamide/2x SSC. Labeled probes were resuspended in 10% (v/v) formamide, 2x SSC, 1 mg ml^{-1} BSA, 10 mM VRC (NEB #S1402S), 5 mM NaHPO4, pH7.5, 0.5 mg ml^{-1} Escherichia coli tRNA and 0.5 mg ml^{-1} single-stranded DNA and hybridized overnight at 37°C. Cells were then washed in 10% formamide/2x SSC at 37°C for 1 hour, followed by a quick wash in 1x PBS at room temperature. The coverslips were quickly dried in 100% ethanol and mounted on glass slides using Prolong Gold with DAPI mounting media (Invitrogen #P36935). For a more detailed protocol see [36,38].

Image acquisition and analysis

Images were acquired using an epifluorescence microscope, either a Nikon E800 upright microscope equipped with a Photometrics CoolSNAP HQ (CCD) camera or a Zeiss Axio Observer Z1 inverse microscope with a Zeiss AxioCam MRm camera, using a 100x oil objective and specific filter cubes (Chroma Filters 31000 (DAPI), 41001 (FITC), SP-102v1 (Cy3/DyLight550), SP-103v1 (Cy3.5/DyLight594), and CP-104 (Cy5/DyLight650) (Chroma Technology, Rockingham, VT)) corresponding to the excitation and emission spectra of the smFISH probes used. 3D image datasets were acquired, with 200mn z-stacks covering the entire depth of cells. The z-stacks were projected onto a 2D plane by applying a maximum projection using ImageJ. RNA signals were detected and quantified using a spot

detection algorithm fitting a 2D Gaussian mask implemented with custom-made software for the IDL platform (ITT Visual Information Solutions); cell and nuclear segmentation as well as quantification of nascent RNAs were performed all as described in [36]. For all quantifications, data from at least 3 different experiments were analyzed, each containing >100 cells. Error bars correspond to standard deviations.

Plasmid constructions

The *PHO84* plasmid with the mutated Nrd1/Nab3 motifs was obtained by first cloning the *PHO84* wild-type gene (−1000bp to +350bp) as a SalI fragment into pUC18 to create pFS3594. A BglII-Nde1 DNA fragment spanning the *PHO84* 3′ end and downstream vector sequences was synthesized by mutagenizing the putative Nrd1/Nab3 binding motifs encoded within the *PHO84* 3′ end on the antisense strand. The wild-type BglII-Nde1 fragment of pFS3521 was replaced by the synthetic mutant fragment to create pFS3644. Both the wild-type and mutant *PHO84* genes were subcloned into YCpLac111 as SalI fragments to generate pFS3521 and pFS3625 respectively.

Northern blot analysis and RT-qPCR

Total RNA was prepared and analysed by Northern blot using standard methods as described [34]. For quantitative RT-PCR quantifications, total RNA was treated with DNase (Ambion) to remove genomic DNA contamination. cDNAs of sense or antisense RNAs were generated by SuperScript II reverse transcriptase (Invitrogen) with 1μg of DNase treated total RNA using gene and strand-specific primers. cDNAs were quantified by real-time qPCR (BioRad). The same amplicon was used to quantify sense and antisense cDNA. The sequences of all the primers are listed in Supplementary Table 2.

Chromatin immunoprecipitation

Chromatin immunoprecipitations (ChIPs) were performed essentially as described previously [34]. Yeast strains were grown to OD_{600} = 0.8 in YEPD medium at 25°C and crosslinked for 10 min by the addition of formaldehyde to a final concentration of 1.2%. Crosslinked and sonicated chromatin extracts from 1.5 mg of Bradford quantified proteins were immunoprecipitated overnight in the presence of protein G Sepharose (Amersham, Pharmacia) with 5 μl of antibody against H3K4me3 (Abcam 8580), H3K4me2 (Abcam 32356), H3 (Abcam 1791, clone Y47), or HA epitope (Covance monoclonal antibody HA. 11, clone 16B12) for the Nrd1-HA tagged strains. All immunoprecipitations were repeated at least three times with different chromatin extracts from independent cultures. Immunoprecipitated DNA was purified and quantified by real-time PCR with primers listed in Supplementary Table 2 and expressed as the percent of input DNA or percent of input DNA normalized to H3. Error bars correspond to standard deviations.

Determination of decay rates

Cells were grown to an OD_{600}=0.8 in YEPD medium. At T=0, 100μg/ml of 1,10 phenanthroline (Sigma) was added to the culture [42] and references therein. Samples were taken at different time points and analyzed for their RNA expression by RT-qPCR as described above.

Half-lives were calculated by the equation t1/2 = 0.693/k, where k is the rate constant for mRNA decay. Values of each time point are normalized for internal variations with *SCR1* RNA, a control that is still stable at the 30 min time point.

Supplementary Material

Refer to Web version on PubMed Central for supplementary material.

Acknowledgments

We thank T. H. Jensen (Aarhus University, Denmark), D. Libri (Centre National de la Recherche Scientifique, Gif-sur-Yvette, France), A. Morillon (Curie Institute, Paris, France) and D. Tollervey (University of Edinburgh, UK) for strains; K. Weis (University of California, Berkeley) for communicating data before publication, D. Larson (National Cancer Institute, Bethesda, USA) for updates of image analysis software and M. Oeffinger, F. Robert, O. Gahura, A. Maffioletti, C. Dargemont and V. Géli for discussions and critical reading of the manuscript. This work was supported by SystemsX and Novartis fellowships (MC), an EMBO fellowship (EG), the Swiss National Science Foundation (grant no. 31003A_130292), the National Center of Competence in Research “Frontiers in Genetics”, IGE3 and the Canton of Geneva (FS), and the Canadian Institutes of Health Research (MOP-BMB-232642), the Canadian Foundation for Innovation and the ‘Fonds de recherche du Québec – Santé’ (Chercheur Boursier Junior I) (DZ).

References

1. Neil H, et al. Widespread bidirectional promoters are the major source of cryptic transcripts in yeast. Nature. 2009; 457:1038–42. [PubMed: 19169244]
2. David L, et al. A high-resolution map of transcription in the yeast genome. Proc Natl Acad Sci U S A. 2006; 103:5320–5. [PubMed: 16569694]
3. Xu Z, et al. Bidirectional promoters generate pervasive transcription in yeast. Nature. 2009; 457:1033–7. [PubMed: 19169243]
4. Jacquier A. The complex eukaryotic transcriptome: unexpected pervasive transcription and novel small RNAs. Nat Rev Genet. 2009; 10:833–44. [PubMed: 19920851]
5. Houseley J, Tollervey D. The many pathways of RNA degradation. Cell. 2009; 136:763–76. [PubMed: 19239894]
6. LaCava J, et al. RNA degradation by the exosome is promoted by a nuclear polyadenylation complex. Cell. 2005; 121:713–24. [PubMed: 15935758]
7. Thiebaut M, Kisseleva-Romanova E, Rougemaille M, Boulay J, Libri D. Transcription termination and nuclear degradation of cryptic unstable transcripts: a role for the nrd1-nab3 pathway in genome surveillance. Mol Cell. 2006; 23:853–64. [PubMed: 16973437]
8. Vanacova S, et al. A new yeast poly(A) polymerase complex involved in RNA quality control. PLoS Biol. 2005; 3:e189. [PubMed: 15828860]
9. Wyers F, et al. Cryptic pol II transcripts are degraded by a nuclear quality control pathway involving a new poly(A) polymerase. Cell. 2005; 121:725–37. [PubMed: 15935759]
10. Arigo JT, Eyler DE, Carroll KL, Corden JL. Termination of cryptic unstable transcripts is directed by yeast RNA-binding proteins Nrd1 and Nab3. Mol Cell. 2006; 23:841–51. [PubMed: 16973436]
11. Vasiljeva L, Buratowski S. Nrd1 interacts with the nuclear exosome for 3′ processing of RNA polymerase II transcripts. Mol Cell. 2006; 21:239–48. [PubMed: 16427013]
12. Carroll KL, Ghirlando R, Ames JM, Corden JL. Interaction of yeast RNA-binding proteins Nrd1 and Nab3 with RNA polymerase II terminator elements. Rna. 2007; 13:361–73. [PubMed: 17237360]
13. Steinmetz EJ, Conrad NK, Brow DA, Corden JL. RNA-binding protein Nrd1 directs poly(A)-independent 3′-end formation of RNA polymerase II transcripts. Nature. 2001; 413:327–31. [PubMed: 11565036]

14. Gudipati RK, Villa T, Boulay J, Libri D. Phosphorylation of the RNA polymerase II C-terminal domain dictates transcription termination choice. Nat Struct Mol Biol. 2008; 15:786–94. [PubMed: 18660821]
15. Kim H, et al. Gene-specific RNA polymerase II phosphorylation and the CTD code. Nat Struct Mol Biol. 2010; 17:1279–86. [PubMed: 20835241]
16. Vasiljeva L, Kim M, Mutschler H, Buratowski S, Meinhart A. The Nrd1-Nab3-Sen1 termination complex interacts with the Ser5-phosphorylated RNA polymerase II C-terminal domain. Nat Struct Mol Biol. 2008; 15:795–804. [PubMed: 18660819]
17. Xu Z, et al. Antisense expression increases gene expression variability and locus interdependency. Mol Syst Biol. 2011; 7:468. [PubMed: 21326235]
18. Murray SC, et al. A pre-initiation complex at the 3′-end of genes drives antisense transcription independent of divergent sense transcription. Nucleic Acids Res. 2011; 40:2432–44. [PubMed: 22123739]
19. Tisseur M, Kwapisz M, Morillon A. Pervasive transcription - Lessons from yeast. Biochimie. 2011; 93:1889–96. [PubMed: 21771634]
20. Hainer SJ, Pruneski JA, Mitchell RD, Monteverde RM, Martens JA. Intergenic transcription causes repression by directing nucleosome assembly. Genes Dev. 2011; 25:29–40. [PubMed: 21156811]
21. Martens JA, Laprade L, Winston F. Intergenic transcription is required to repress the Saccharomyces cerevisiae SER3 gene. Nature. 2004; 429:571–4. [PubMed: 15175754]
22. Thiebaut M, et al. Futile cycle of transcription initiation and termination modulates the response to nucleotide shortage in S. cerevisiae. Molecular Cell. 2008; 31:671–82. [PubMed: 18775327]
23. Bumgarner SL, et al. Single-cell analysis reveals that noncoding RNAs contribute to clonal heterogeneity by modulating transcription factor recruitment. Mol Cell. 2012; 45:470–82. [PubMed: 22264825]
24. van Werven FJ, et al. Transcription of Two Long Noncoding RNAs Mediates Mating-Type Control of Gametogenesis in Budding Yeast. Cell. 2012
25. Gelfand B, et al. Regulated antisense transcription controls expression of cell-type-specific genes in yeast. Mol Cell Biol. 2011; 31:1701–9. [PubMed: 21300780]
26. Hongay CF, Grisafi PL, Galitski T, Fink GR. Antisense Transcription Controls Cell Fate in Saccharomyces cerevisiae. Cell. 2006; 127:735–745. [PubMed: 17110333]
27. Houseley J, Rubbi L, Grunstein M, Tollervey D, Vogelauer M. A ncRNA modulates histone modification and mRNA induction in the yeast GAL gene cluster. Mol Cell. 2008; 32:685–95. [PubMed: 19061643]
28. Pinskaya M, Gourvennec S, Morillon A. H3 lysine 4 di- and tri-methylation deposited by cryptic transcription attenuates promoter activation. Embo J. 2009; 28:1697–707. [PubMed: 19407817]
29. Kim T, Xu Z, Clauder-Munster S, Steinmetz LM, Buratowski S. Set3 HDAC Mediates Effects of Overlapping Noncoding Transcription on Gene Induction Kinetics. Cell. 2012
30. Weiner A, et al. Systematic dissection of roles for chromatin regulators in a yeast stress response. PLoS Biol. 2012; 10:e1001369. [PubMed: 22912562]
31. Komeili A, O'Shea EK. Roles of phosphorylation sites in regulating activity of the transcription factor Pho4. Science. 1999; 284:977–80. [PubMed: 10320381]
32. Lam FH, Steger DJ, O'Shea EK. Chromatin decouples promoter threshold from dynamic range. Nature. 2008; 453:246–50. [PubMed: 18418379]
33. Wippo CJ, et al. Differential cofactor requirements for histone eviction from two nucleosomes at the yeast PHO84 promoter are determined by intrinsic nucleosome stability. Mol Cell Biol. 2009; 29:2960–81. [PubMed: 19307305]
34. Camblong J, Iglesias N, Fickentscher C, Dieppois G, Stutz F. Antisense RNA stabilization induces transcriptional gene silencing via histone deacetylation in S. cerevisiae. Cell. 2007; 131:706–17. [PubMed: 18022365]
35. Femino AM, Fay FS, Fogarty K, Singer RH. Visualization of single RNA transcripts in situ. Science. 1998; 280:585–90. [PubMed: 9554849]
36. Zenklusen D, Larson DR, Singer RH. Single-RNA counting reveals alternative modes of gene expression in yeast. Nat Struct Mol Biol. 2008; 15:1263–71. [PubMed: 19011635]

37. Raj A, van den Bogaard P, Rifkin SA, van Oudenaarden A, Tyagi S. Imaging individual mRNA molecules using multiple singly labeled probes. Nat Methods. 2008; 5:877–9. [PubMed: 18806792]
38. Zenklusen D, Singer RH. Analyzing mRNA expression using single mRNA resolution fluorescent in situ hybridization. Methods Enzymol. 2010; 470:641–59. [PubMed: 20946829]
39. Oeffinger M, Zenklusen D. To the pore and through the pore: A story of mRNA export kinetics. Biochim Biophys Acta. 2012; 1819:494–506. [PubMed: 22387213]
40. Rougemaille M, et al. Dissecting mechanisms of nuclear mRNA surveillance in THO/sub2 complex mutants. EMBO J. 2007; 26:2317–26. [PubMed: 17410208]
41. Nonet M, Scafe C, Sexton J, Young R. Eucaryotic RNA polymerase conditional mutant that rapidly ceases mRNA synthesis. Mol Cell Biol. 1987; 7:1602–11. [PubMed: 3299050]
42. Grigull J, Mnaimneh S, Pootoolal J, Robinson MD, Hughes TR. Genome-wide analysis of mRNA stability using transcription inhibitors and microarrays reveals posttranscriptional control of ribosome biogenesis factors. Mol Cell Biol. 2004; 24:5534–47. [PubMed: 15169913]
43. Krogan NJ, et al. The Paf1 complex is required for histone H3 methylation by COMPASS and Dot1p: linking transcriptional elongation to histone methylation. Mol Cell. 2003; 11:721–9. [PubMed: 12667454]
44. Ng HH, Robert F, Young RA, Struhl K. Targeted recruitment of Set1 histone methylase by elongating Pol II provides a localized mark and memory of recent transcriptional activity. Mol Cell. 2003; 11:709–19. [PubMed: 12667453]
45. Creamer TJ, et al. Transcriptome-wide binding sites for components of the Saccharomyces cerevisiae non-poly(A) termination pathway: Nrd1, Nab3, and Sen1. PLoS Genet. 2011; 7:e1002329. [PubMed: 22028667]
46. Wlotzka W, Kudla G, Granneman S, Tollervey D. The nuclear RNA polymerase II surveillance system targets polymerase III transcripts. Embo J. 2011; 30:1790–803. [PubMed: 21460797]
47. Soares LM, Buratowski S. Yeast Swd2 Is Essential Because of Antagonism between Set1 Histone Methyltransferase Complex and APT (Associated with Pta1) Termination Factor. J Biol Chem. 2012; 287:15219–31. [PubMed: 22431730]
48. Camblong J, et al. Trans-acting antisense RNAs mediate transcriptional gene cosuppression in S. cerevisiae. Genes Dev. 2009; 23:1534–45. [PubMed: 19571181]
49. Margaritis T, et al. Two distinct repressive mechanisms for histone 3 lysine 4 methylation through promoting 3′-end antisense transcription. PLoS Genet. 2012; 8:e1002952. [PubMed: 23028359]
50. Grzechnik P, Kufel J. Polyadenylation linked to transcription termination directs the processing of snoRNA precursors in yeast. Mol Cell. 2008; 32:247–58. [PubMed: 18951092]
51. Gudipati RK, et al. Extensive Degradation of RNA Precursors by the Exosome in Wild-Type Cells. Mol Cell. 2012; 48:409–421. [PubMed: 23000176]
52. Darby MM, Serebreni L, Pan X, Boeke JD, Corden JL. The S. cerevisiae Nrd1-Nab3 Transcription Termination Pathway Acts in Opposition to Ras Signaling and Mediates Response to Nutrient Depletion. Mol Cell Biol. 2012; 32:1762–1775. [PubMed: 22431520]
53. Lardenois A, et al. Execution of the meiotic noncoding RNA expression program and the onset of gametogenesis in yeast require the conserved exosome subunit Rrp6. Proc Natl Acad Sci U S A. 2011; 108:1058–63. [PubMed: 21149693]
54. van Dijk EL, et al. XUTs are a class of Xrn1-sensitive antisense regulatory non-coding RNA in yeast. Nature. 2011; 475:114–7. [PubMed: 21697827]
55. Buratowski S, Kim T. The role of cotranscriptional histone methylations. Cold Spring Harb Symp Quant Biol. 2010; 75:95–102. [PubMed: 21447819]
56. Holstege FC, et al. Dissecting the regulatory circuitry of a eukaryotic genome. Cell. 1998; 95:717–28. [PubMed: 9845373]
57. Wang Y, et al. Precision and functional specificity in mRNA decay. Proc Natl Acad Sci U S A. 2002; 99:5860–5. [PubMed: 11972065]
58. Jimeno S, Rondon AG, Luna R, Aguilera A. The yeast THO complex and mRNA export factors link RNA metabolism with transcription and genome instability. Embo J. 2002; 21:3526–35. [PubMed: 12093753]

59. Houseley J, Tollervey D. Yeast Trf5p is a nuclear poly(A) polymerase. EMBO Rep. 2006; 7:205–11. [PubMed: 16374505]

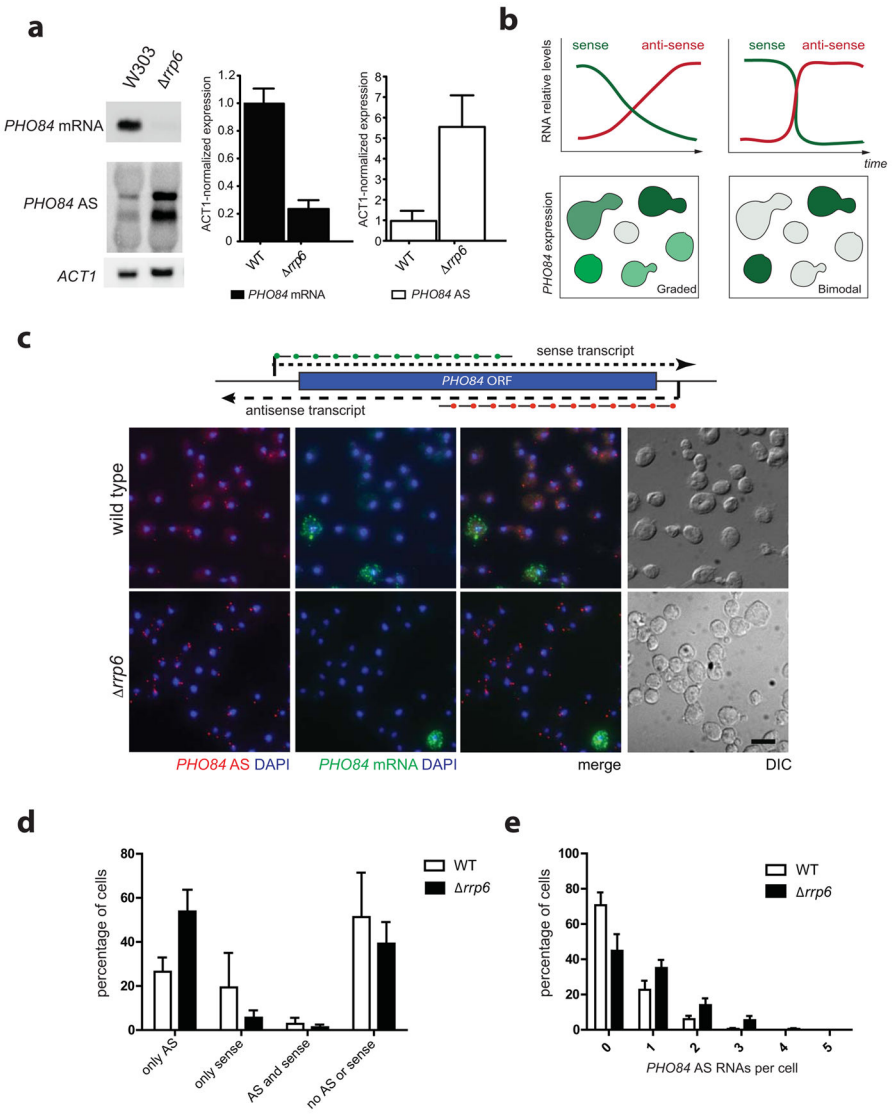

Figure 1. *PHO84* sense and antisense expression are anti-correlated

(a) Deletion of *RRP6* increases expression of *PHO84* antisense RNA. Northern blot (left) and RT-qPCR (right) analyses in WT and *Δrrp6*. Error bars reflect standard deviations of an average from 3 independent experiments. **(b)** Two possible models for antisense-mediated gene silencing. In a graded response, gradual accumulation of *PHO84* AS RNAs leads to a gradual reduction in sense levels (Top left), whereas in a bimodal response, sense and antisense expression are anti-correlated (Top right). Changes in *PHO84* mRNA and antisense levels over time are represented as green and red lines respectively. Lower panels show *PHO84* sense expression resulting from graded or bimodal regulation at the single cell level. **(c)** Bimodal expression of *PHO84* sense and antisense RNAs. smFISH detects *PHO84* sense (green) and antisense RNAs (red) in individual WT and *Δrrp6* cells. Nuclear DNA was stained using DAPI (blue), cellular outlines were visualized using DIC optics and the scale bar is 5μm. FISH probes positions are drawn at the top. **(d)** Less cells express *PHO84* sense in *Δrrp6*. Frequency distribution of *PHO84* sense and AS expression in individual cells from

(**c**). **(e)** Deletion of *RRP6* results in higher level of *PHO84* AS RNA in single cells. Frequency distribution of the number of *PHO84* AS RNAs per cell in WT and *Δrrp6*. Error bars in (**d**) and (**e**) reflect standard deviations of an average of three independent experiments.

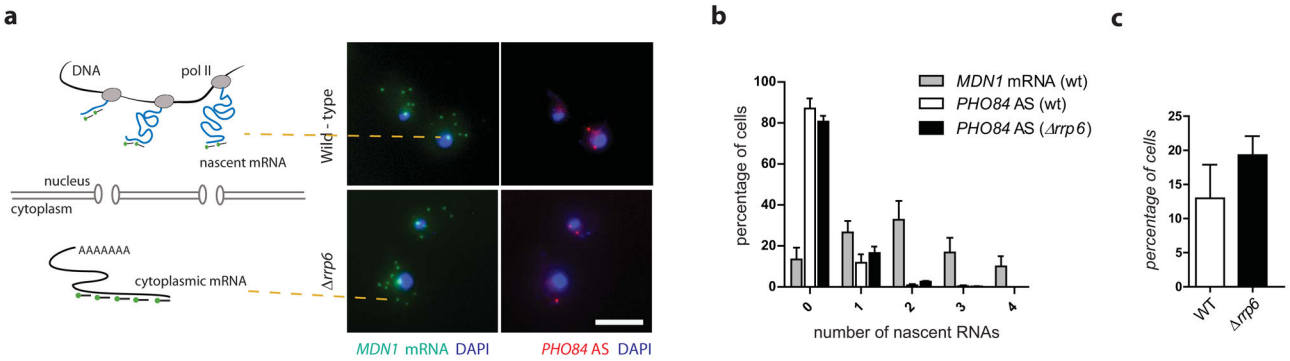

Figure 2. *PHO84* antisense RNAs do not accumulate at the *PHO84* locus

(a) *PHO84* AS RNAs are exported to the cytoplasm. smFISH for *MDN1* mRNA (green) and *PHO84* AS RNA (red) in WT and *Δrrp6* cells. Scale bar is 5μm. The cartoon on the left illustrates the detection of nascent and cytoplasmic RNAs. **(b)** *PHO84* AS RNAs do not accumulate at the *PHO84* gene locus. Frequency distribution of the number of nascent RNAs for *MDN1* (WT only) and *PHO84* AS RNAs in WT and *Δrrp6*. **(c)** Deletion of *RRP6* leads to a higher frequency of cells showing nascent *PHO84* AS RNAs. Frequency distribution of cells containing nascent (nuclear) *PHO84* AS RNAs in WT and *Δrrp6.* Error bars in (**b**) and (**c**) reflect standard deviations of an average of three independent experiments.

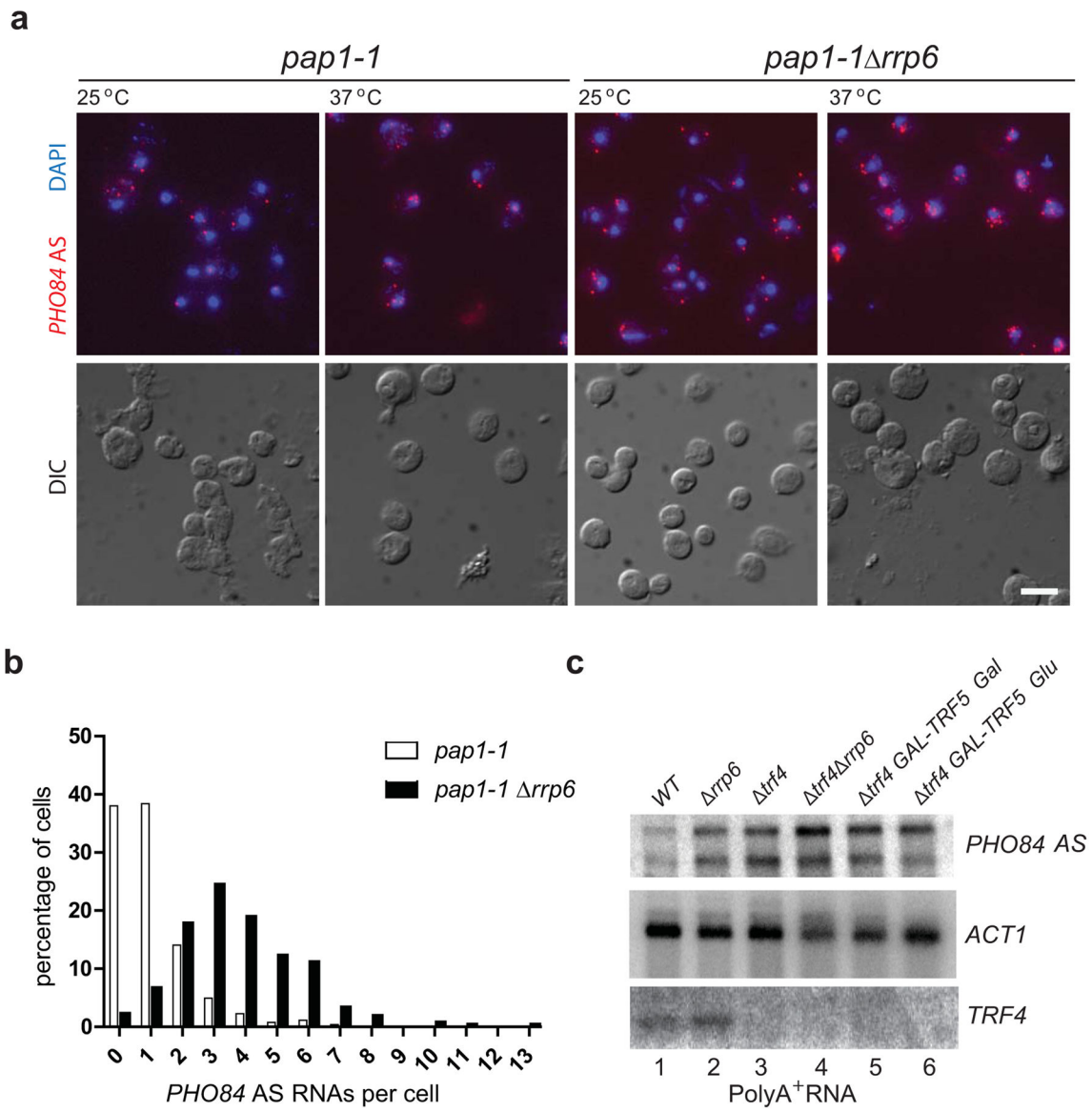

Figure 3. *PHO84* antisense RNAs are polyadenylated by Pap1

(a) Inactivation of Pap1 leads to nuclear accumulation of *PHO84* AS RNAs. smFISH using probes against *PHO84* AS RNAs (red) in *pap1-1* and *pap1-1Δrrp6* cells grown at 25°C and either directly fixed or shifted to 37°C for 1 hour prior to fixation. Nuclear DNA was stained using DAPI (blue), cellular outlines were visualized using DIC optics and the scale bar is 5μm. **(b)** *pap1-1Δrrp6* cells accumulate high numbers of *PHO84* AS RNA in the nucleus. Frequency distribution of the number of *PHO84* AS RNAs detected by smFISH in *pap1-1* and *pap1-1Δrrp6* cells after 1 hour shift to 37°C. **(c)** *PHO84* AS RNAs polyadenylation requires Pap1. Northern blot membranes with oligo dT purified total RNA were hybridized with *PHO84* AS specific probes. Strains were exponentially grown in SC medium 2% glucose (Glu; lanes 1–4) or 2% galactose (Gal; lane 5) followed by 20h in 2% glucose (Glu; lane 6) to deplete Trf5 as indicated. *ACT1* and *TRF4* mRNA specific probes were used to control for loading and *TRF4* deletion.

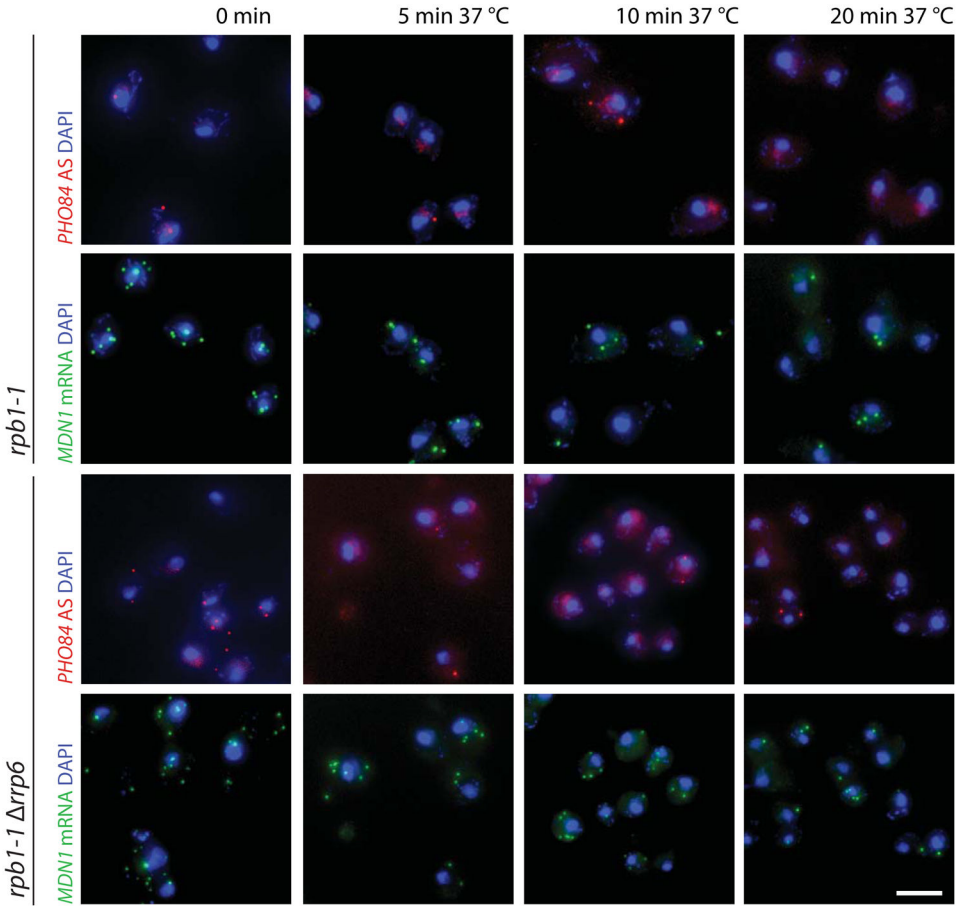

Figure 4. *PHO84* antisense nuclear detection needs ongoing transcription

smFISH detecting *MDN1* mRNA (green) and *PHO84* AS RNA (red) in *rpb1-1* and *rpb1-1Δrrp6* cells grown at 25°C and shifted to 37°C for 5, 10 and 20 min prior to fixation. Nuclear DNA was stained using DAPI (blue), cellular outlines were visualized using DIC optics and the scale bar is 5μm.

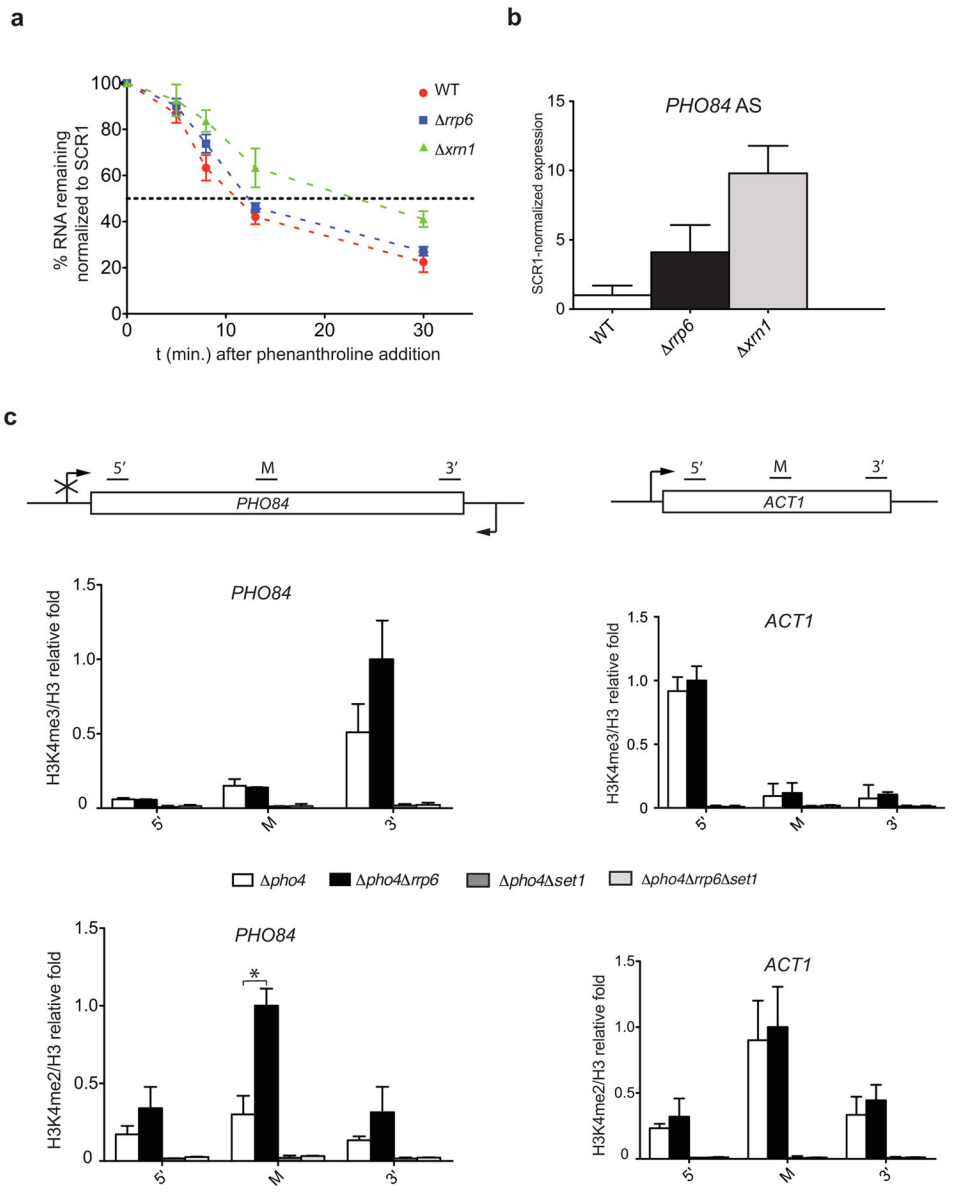

Figure 5. Effect of Δ*rrp6* on antisense RNA half-life and transcription

(a) Deletion of *RRP6* does not alter *PHO84* AS RNA half-life. RT-PCR analysis measuring *PHO84* AS RNA decay rates in WT, *Δrrp6* and *Δxrn1* after transcription shut off by adding 100 μg/ml 1, 10-Phenantroline to the medium. *PHO84* AS RNA levels were normalized to *SCR1* RNA, stable at 30 min. Data are expressed as a percentage of the amounts present before addition of the inhibitor. Error bars represent standard deviations for three independent experiments. **(b)** *PHO84* AS RNA levels are elevated in a *Δrrp6* and *Δxrn1.* Antisense RNA levels were measured by RT-qPCR and expressed relative to the levels in WT that were set to 1. Error bars reflect standard deviations of an average obtained from three independent experiments. **(c)** Higher levels of H3K4 tri- and di-methylation at the 3′ end of *PHO84* in *Δrrp6.* Chromatin immunoprecipitation (ChIP) analysis of H3K4 tri- (top) and di-methylation (bottom) at the *PHO84* locus. ChIP with anti-H3K4me3, anti-H3K4me2

or anti-H3 antibodies from *Δpho4, Δpho4Δrrp6, Δpho4Δset1* and *Δpho4Δrrp6Δset1* strains. DNA quantified by real-time PCR with primers specific for the 5′, middle and 3′ regions of *PHO84* and *ACT1* (as indicated on top). H3K4me2/3 values were normalized to H3 values and the highest value was arbitrarily set to 1. Error bars reflect standard deviations of an average obtained from three independent experiments. Comparison of the mean differences was analysed by the Student-t test. P values <0.05 are indicated by (*).

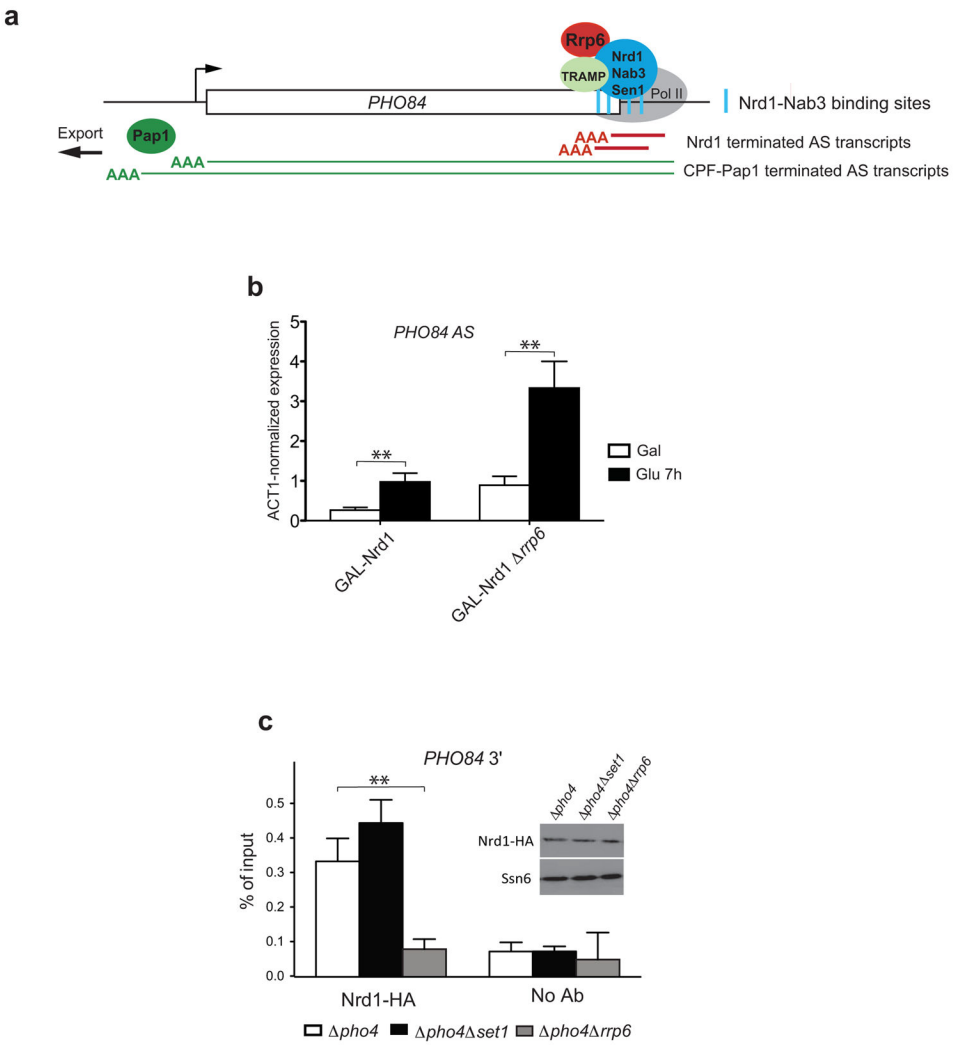

Figure 6. *PHO84* antisense transcription is attenuated by NNS

(a) NNS terminates short *PHO84* AS transcripts. Cartoon illustrating the role of NNS in *PHO84* AS transcription. Short antisense RNAs (red line) previously shown to be polyadenylated by Trf4 and degraded by Rrp6 [1] are proposed here to be terminated at Nrd1-Nab3 motifs (blue bars) by the NNS complex, while the long read-through antisense transcripts (green lines) are subjected to 3′end cleavage and polyadenylation by Pap1 before export into the cytoplasm. **(b)** Depletion of Nrd1 increases *PHO84* AS RNA levels. *PHO84* AS RNA levels were measured using RT-qPCR after in GAL-Nrd1 and GAL-Nrd1 *Δrrp6* strains grown in medium containing 2% galactose (Gal) or shifted for 7h in 2% glucose (Glu) to deplete Nrd1. Error bars reflect standard deviations of an average from 3 independent experiments. Comparison of the mean differences was analysed by the Student-t test. Stars indicate the level of significance: p value <0.01 (**). The value of GAL-Nrd1 (Glu 7h) was arbitrarily set to 1. **(c)** Deletion of *RRP6* reduces Nrd1 recruitment. ChIP analysis of Nrd1-HA binding at *PHO84* 3′ end quantified by qPCR and expressed as % of input. Three biological and two technical repeats were analysed, error bars reflect standard errors. Comparison of the mean differences was analysed by the Student-t test. Stars indicate

the level of significance: p value <0.01 (**). The small panel shows Western blot analysis of Nrd1 protein levels in the strains used for the ChIP. Ssn6 was used as normalization control.